

## Positive and Negative Contrast Lithography on Silver Quantum Dot Monolayers

Sven E. Henrichs, Jennifer L. Sample, Joe J. Shiang, and James R. Heath\*

UCLA Department of Chemistry and Biochemistry, 405 Hilgard, Los Angeles, California 90095-1569

Charles P. Collier and Richard J. Saykally

Department of Chemistry, University of California, Berkeley, California 94720-1460

Received: January 6, 1999; In Final Form: March 1, 1999

Scanning nonlinear optical microscopy, at a resolution of  $\sim 2 \mu\text{m}$ , was utilized to examine monolayers of alkythiol-passivated silver nanocrystals. Selected regions of the monolayers were irradiated with a pulse train of picosecond 1064 nm laser pulses, and then the second harmonic generation (SHG) response of those monolayers was recorded in a second scan. Two lithographic processes—one leading to a negative contrast SHG image (observed for particles  $< 4 \text{ nm}$  diameter) and a second leading to a positive contrast SHG image (observed for larger particles)—were found. These processes are explained within the context of literature models that account for particle size dependent energy partitioning.

### Introduction

Nanometer sized particles of coinage metals are prototypes for the investigation of finite size phenomena in metals. Not only are these particles simple to prepare and handle, also but they are characterized by a strong (collective) optical resonance, known as a surface plasmon ( $\omega_{\text{sp}}$ ). The resonance frequency, peak width, and intensity are sensitive indicators of particle size, shape, and chemical environment.<sup>1,2</sup> In this paper, we report on investigations of monolayers of various sized alkythiol-passivated silver nanocrystals using a scanning nonlinear optical microscope (SNLOM), operating at  $\lambda = 1064 \text{ nm}$  and a spatial resolution of  $\sim 2 \mu\text{m}^2$ . The monolayers were supported on a glass substrate and covered with a thin film of ethylene glycol. Depending on the size of the particles, we found two distinct optical responses, and these responses lead to mechanisms for negative and positive contrast optical lithography. For small nanocrystals ( $< 4 \text{ nm}$  diameter), we found evidence for strong coupling of electronic excitation to translational (thermal) motion. The second harmonic generation (SHG) response of these films was reduced in regions that were previously irradiated (written), leading to a negative contrast scanning SHG image of the surface. Larger particles were observed to ionize through a high order multiphoton process. We postulate that the effect of this “writing” process was to generate a local field at the nanocrystal/ethylene glycol interface, which, in turn, activated a  $\chi^3$  process at  $\lambda/2$ . For those films, a high positive contrast scanning SHG image was observed for a previously irradiated film. These results are discussed within the context of literature reports of particle size dependent electronic relaxation rates.

### Experimental Section

The preparation and size-selection of alkythiol-passivated Ag nanocrystals has been reported.<sup>3</sup> Particle sizes were determined by one or more of the following: UV/vis absorption spectroscopy, transmission electron microscopy, and X-ray powder

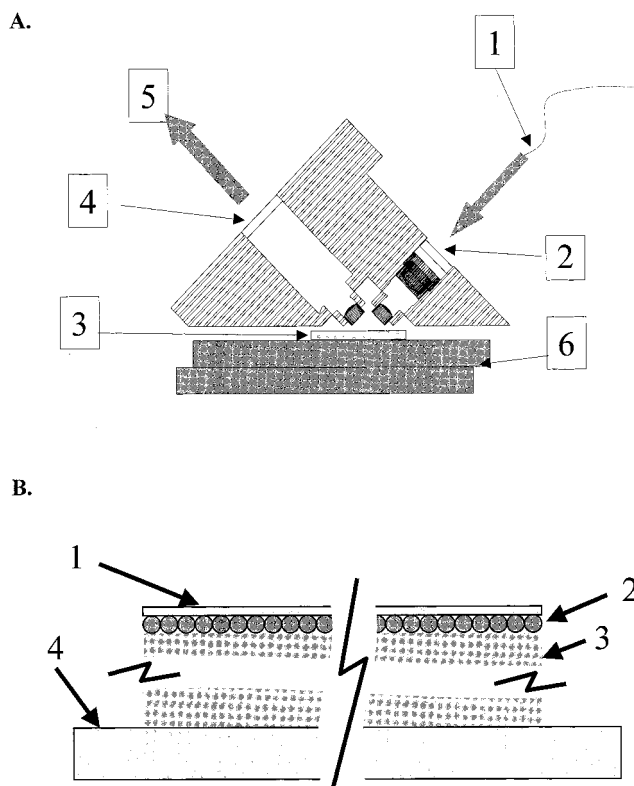


**Figure 1.** (A) Cross-sectional view of the scanning nonlinear optical microscope. The light is fed into the microscope using a single mode optical fiber [1], and focused through a series of optics and filters to a  $\sim 2 \mu\text{m}$  diameter spot size on the substrate [3]. The reflected light is collimated and filtered [4] and directed to a photomultiplier tube [5]. The sample is scanned underneath the microscope using x- and y-piezoelectric translation stages [6]. The sample (B) consists of a glass coverslip [1] coated with a monolayer of silver quantum dots [2], a thin film of ethylene glycol [3], and supported on a second glass cover slip [4].

diffraction. The size distribution widths of the particles were typically about  $\pm 10\% = 2\sigma$  of the quoted particle size. The

\* Author to whom correspondence should be addressed.

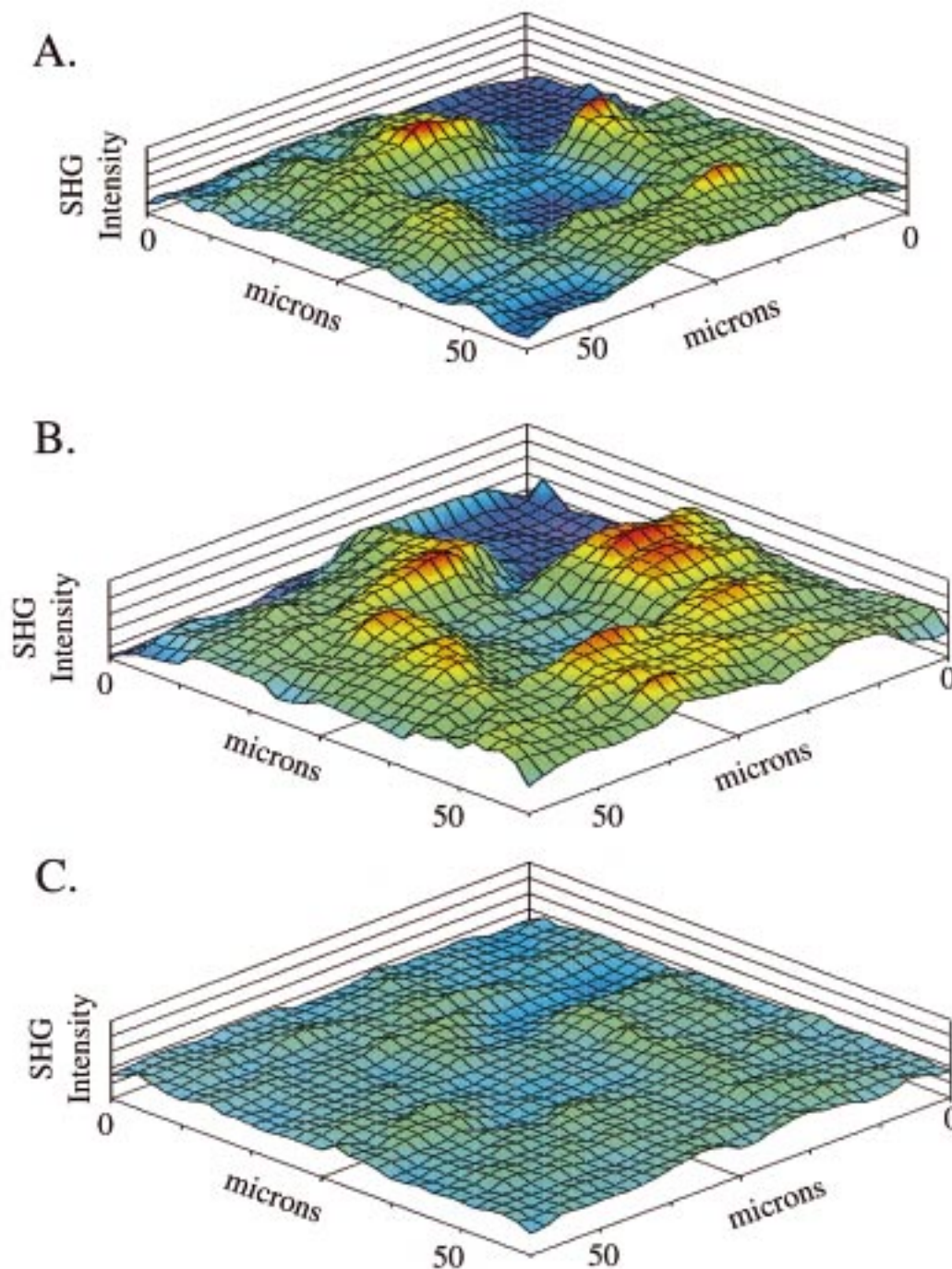


**Figure 2.** Scanning SHG (*read* step) micrographs of monolayers of (A) 2.5, (B) 3.5, and (C) *chemically linked* 2.5 nm diameter dodecanethiol passivated Ag nanocrystals. For all images, three  $100 \mu\text{m}^2$  square regions (from top left corner and across the diagonal of the images) had been previously irradiated (*written*) at a level of 20, 10, and 5 laser shots per scan step ( $2 \mu\text{m}$  diameter spot size). In both (A) and (B), the measured SHG response is inversely proportional to the amount of exposure in the write step, and an increased SHG response is observed at the perimeters of the previously written regions. In (C), the write step had no effect on the particle monolayer, indicating that, for the unlinked particles, the energy absorbed during the write step is converted to translational energy, and the particles are moved away from the written areas.

nanocrystals were prepared as a Langmuir monolayer and transferred as a Langmuir–Schaeffer film to a glass cover slip, as described previously.<sup>3</sup> A drop of ethylene glycol was placed on top of the monolayer, and the particle/ethylene glycol films were covered with a second cover slip.

A diagram of the SNLOM, which used a mode-locked, pulsed Nd:YAG laser illumination source (1064 nm, 50 ps pulse train at 10 Hz,  $\sim 0.5 \mu\text{J}/\text{pulse}$ ), is shown in Figure 1A. The laser was coupled into the lens system with a single-mode optical fiber, passed through a polarizer, and then focused onto the sample at a  $45^\circ$  angle to a minimum diffraction limited spot size of

about  $2 \mu\text{m}$  diameter. The lenses are aspheric molded gel lenses, which are small-diameter lenses with high numerical apertures. The reflected light was then collimated by another lens, the fundamental laser was filtered out with short pass filters, and the SHG signal was detected with an amplified photomultiplier tube. The incident laser fluence was controlled by a series of neutral density filters before the input to the fiber optic. Although the fluence was low, the short pulse width, coupled with the small area focus, implies a peak incident power of  $\sim 10^{11} \text{ W}/\text{cm}^2$ . The sample was mounted on a pair of inchworm piezoelectric stages for  $x$  and  $y$  translation, and scanned beneath

the laser spot. An image was constructed from the collected signal. All images presented here were made by first scanning a small area (the *write* step), then reducing the power and scanning a larger area (the *read* step), which included the original area, to image the effects of the write step. All results shown were for p-input polarization and unpolarized, filtered detection of the output SHG.

A diagram of the sample is shown in Figure 1B. With no ethylene glycol, the laser damaged (presumably metallized) the film, and the SHG signal strongly decreased after a couple of laser shots. Samples with the ethylene glycol gave a steady SHG signal that persisted for several seconds when a single spot was irradiated. Except where noted, the signal collected by the microscope was SHG at 532 nm as confirmed by inserting various long and short pass filters into the signal path.

The plasmon,  $\omega_{sp}$ , causes a resonant enhancement of nonlinear optical signals in the visible part of the spectrum, given the appropriate optical geometry.<sup>4</sup> SHG is a second order ( $\chi^{(2)}$ ) nonlinear process which, in the electric dipole approximation, requires a breaking of the symmetry in the SHG medium for any second harmonic light to be produced. However, in order for the polarization vector of the incident light to sample the asymmetry at the interface, the light must be incident on the surface at a large angle relative to the surface normal.<sup>5</sup> One example of SHG microscopy uses a pulsed YAG laser as the illumination source in a traditional microscope, where the direction of propagation of the incident laser is parallel to the surface normal.<sup>6</sup> This geometry is sensitive to the orientations of noncentrosymmetric crystalline domains within the plane of the film, but not the asymmetry across the thin film interface. We observed no SHG signal from our system in this geometry because the relevant  $\chi^{(2)}$  tensor elements are zero for either hexagonal or isotropically amorphous domains.<sup>7</sup> Scanning imaging techniques and special optics are necessary for achieving high spatial resolution with a high incident angle.<sup>8–11</sup> Our SNLOM achieves a resolution close to the diffraction limit (for 1064 nm radiation) of  $\sim 2 \mu\text{m}^2$  at a geometry for which all nonlinear optical processes are symmetry allowed for a two-dimensional sample.<sup>5,7</sup>

## Results and Discussion

Experimental results for 2.5 and 3.5 nm Ag nanocrystals are shown in Figure 2, parts A and B, respectively. The particles have apparently moved away from the regions that were scanned during the write step, in proportion to the number of laser shots that were used. This effect is less pronounced for larger particles. To confirm that particle motion is responsible for the effects seen in the SHG micrographs, a monolayer of 2.5 nm particles was chemically "linked" by immersing the transferred film in an acetone solution of dodecane dithiol for several minutes. Laser irradiation had little effect on this monolayer (Figure 2C).

We modeled these data by assuming that all of the particles within the laser spot were laser-desorbed from the film, distributed evenly within a hemispherical volume within the ethylene glycol overlayer, and then settled back onto the substrate. Figure 3 shows the results for such a simulation that included a 3  $\mu\text{m}$  diameter irradiated area of particles that desorbed into a 30  $\mu\text{m}$  radius hemispherical volume. The implication is that the energy absorbed by the particles is transferred to the ethylene glycol heat bath, causing local heating and subsequent vaporization of a thin (1–2  $\mu\text{m}$ ) layer of ethylene glycol. On the basis of the heat of vaporization of ethylene glycol, the amount of energy needed to form a 30  $\mu\text{m}$  diameter vapor bubble of ethylene glycol is a few nanojoules.

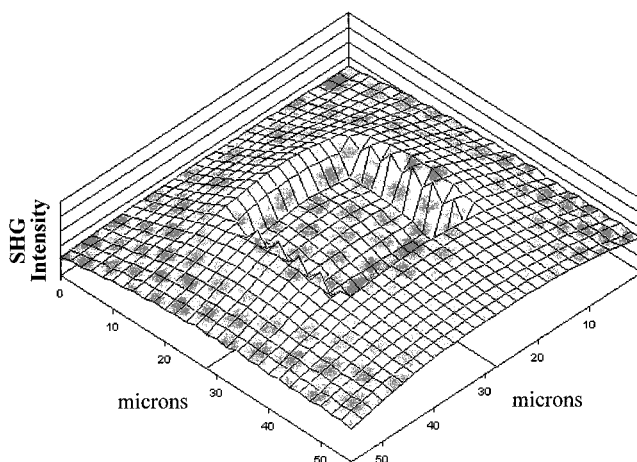


**Figure 3.** Computer simulation of the process shown in Figure 2 (A) and (B). The simulation is based on a model in which the energy adsorbed by the particles is transferred to the ethylene glycol heat bath. A 1–2  $\mu\text{m}$  thick layer of ethylene glycol is vaporized. The particles are pulled into the expanding solvent plume, and then recondense onto a larger spot size on the substrate. Several experimental details are reproduced by the simulation, including an increased SHG response from the areas that surround the written area, as well as an intensity gradient in the SHG signal across the irradiated square itself, in the direction of the scan (back left to front right).

This is just a fraction of a percent of the energy incident on the sample per laser shot, and is consistent with the low absorption efficiency of the particles at 1064 nm. The observation that smaller particles move more readily than larger ones is consistent with the fact that a monolayer of larger particles should be more strongly bound.<sup>12</sup>

For particles larger than about 6 nm, a new process dominates, and the laser power dependence of this process is shown in the nonlinear optical micrograph of Figure 4A. A selected region of the monolayer (top of Figure 4A) was exposed to a focused laser beam at a power of about  $2 \times 10^{11} \text{ W/cm}^2$ . A strong quasi-continuum optical emission, centered near 550 nm, was recorded during this *write* step (Figure 4B). The image was then *read* by reducing the laser power a factor of 2, which is below the threshold for signal in the *write* step, and scanning over a large area that included the written spots. Strongly enhanced SHG signal was observed in the areas that had been previously scanned, while only a weak signal was observed in the unscanned region.

Several experiments were carried out to ascertain the nature of this process. First, the response of a dry film (no ethylene glycol) was measured, and no enhanced signal was observed during the read step. The power dependence of the *write* step (Figure 4A) reveals that the effect is highly nonlinear. The film shows no enhanced SHG response in the read step until the write power is raised to  $\sim 1.5 \times 10^{11} \text{ W/cm}^2$ , above which point the effect of the *write* step quickly saturates. Third, monolayers of several different particle sizes, ranging from  $\sim 50$  to 80  $\text{\AA}$  were probed. For particles between 40 and 60  $\text{\AA}$ , we observed a small amount of movement and a strongly enhanced optical signal. The high-order nonlinear laser power dependence, the particle size dependence, and the continuum emission recorded during the write step all point to a multiphoton ionization (thermionic emission) *write* step.<sup>13</sup> The resulting charged layer can induce a polarization in the ethylene glycol, resulting in an enhanced SHG signal. Zhao, Ong, and Eisenhalt have observed enhanced SHG from ionized organic monolayers, and have attributed that enhancement to a  $\chi^{(3)}$  process.<sup>14</sup> SHG is a  $\chi^{(2)}$  process, meaning that it is based on the second-order hyper-



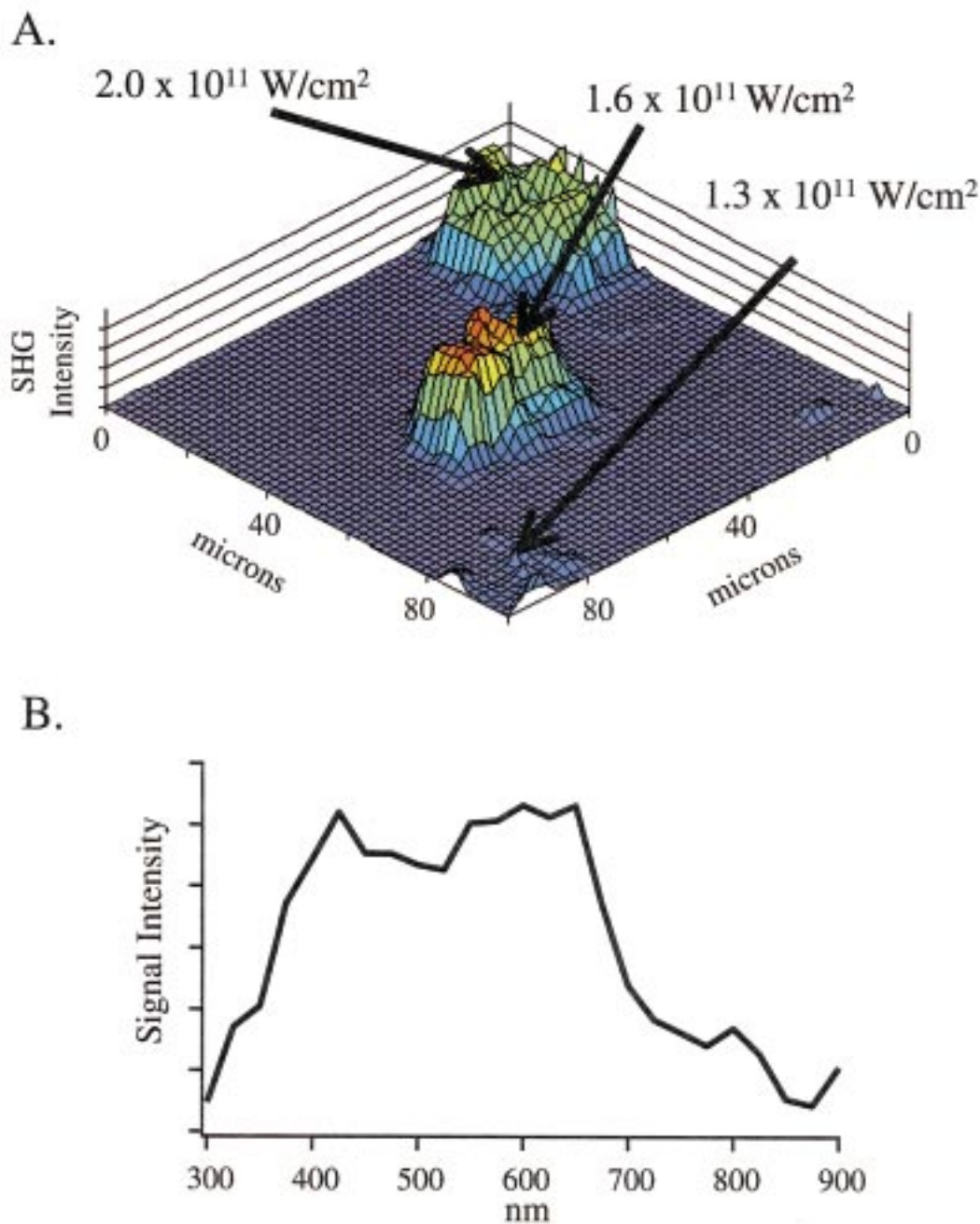


**Figure 4.** Write-step power dependence of the scanning SHG (*read* step) microscopy of monolayers of 6 nm diameter dodecanethiol passivated Ag nanocrystals. In the previous (*write*) step,  $100 \mu\text{m}^2$  areas were irradiated with 10 laser shots per scan step, but with variable laser power as indicated on the figure. At sufficiently high laser pulse energies, a broad (essentially continuous) emission spectrum is recorded during the *write* step (Figure B). The resulting *read* step then reveals that the previously irradiated regions now exhibit a very strongly  $10^2$ – $10^3$  enhanced SHG response. A mechanism that relates this enhanced SHG response to particle ionization is postulated.

polarizability of a material, and requires the presence of two electric fields—i.e., two photons. For  $\chi^{(3)}$  to be activated, a third electric field is necessary, and Eisenthal proposed that this field originated from the static field of the ionized monolayer and the polarized chemical environment. As a final check, microscopic inspection of irradiated areas revealed no sign of damage. In fact, all of the monolayers (except the linked particles of Figure 2c) discussed here could be redissolved as a colloid in hexane or  $\text{HCCl}_3$  after the experiments had been carried out.

Before explaining the size-dependent partitioning of energy that we have observed, we briefly review electron relaxation processes in the particles. The collision rate of electrons in the bulk is  $\nu_f/\xi$ , and is proportional to the bulk plasmon line width. Here,  $\nu_f$  is the Fermi velocity and  $\xi$  is the mean free path of an

electron in bulk silver. In a finite sized crystal, the linewidth becomes a function of the radius ( $r$ ) of the particle, and is

$$\omega_c(r) \propto \left( \frac{1}{\xi} + \frac{1}{r} \right) \nu_f$$

This linewidth is the electronic dephasing rate of the plasmon, and is extremely short ( $< 100$  fs).<sup>15–19</sup> After this initial dephasing period, the particle is left with “hot” electrons. Eventually, these electrons equilibrate with the environment via electron–phonon coupling, thereby heating the particle. However, if energy is continually pumped into the system while the electrons are still hot, laser-induced thermionic emission can occur.<sup>20</sup> Smith and co-workers<sup>21</sup> developed a simple equation to describe the size

dependence of the relaxation of the hot electrons:

$$\frac{1}{\tau_{\text{obs}}} = \frac{ar^\alpha}{\tau_{\text{bulk}}} + \frac{bv_f}{r}$$

Here,  $\tau_{\text{obs}}$  is the observed lifetime of the hot electrons in the particles,  $\tau_{\text{bulk}}$  is the lifetime of the hot electrons in the bulk,  $a$  and  $b$  are material constants, and  $\alpha$  is a positive integer. The density of phonon states drops with decreasing particle size (first term), leading to a drop in electron-phonon coupling, and an increased lifetime of the hot electrons. However, the rate of electron surface scattering (the second term), increases with decreasing size, thereby reducing the lifetime of the hot electrons. The net result is that the hot electron lifetime will initially pass through a maximum as particle size is decreased, and then drops for sufficiently small particles. This trend has been confirmed for Au nanoparticles.<sup>21,22</sup> Assuming that similar physics applies to Ag nanocrystals, we estimate (assuming a bulk hot electron lifetime of  $\sim 0.5$  ps) that the hot electron lifetime for a 10 nm particle is  $\sim 7$  ps, and the lifetime for a 2 nm particle is  $\sim 1$  ps.<sup>23</sup> Both these time scales and particles sizes are relevant to the current experiment.

The data that we present suggest that when the size of the particles is less than  $\sim 5$  nm, the hot electrons relax to an equilibrium state and heat the surroundings before thermionic emission can occur. For larger particles, the lifetime of the hot electrons increases, and these charge carriers continue to absorb energy from the laser pulse until they are ionized. The continuum emission recorded during the write step is likely due to these ionized electrons. As would be expected, the transition between the two mechanisms is a gradual, rather than a sharp, function of particle size.

One appealing aspect of the proposed writing mechanism is that it might be possible to erase the written information by charge neutralization. Experiments in which the ethylene glycol layer can be modified using a liquid flow cell are currently being set up to explore this. If it were possible to erase the data, then this system would represent the only read/write/erase optical storage system that we know of, and should, in addition, scale to extremely small length scales.

**Acknowledgment.** S.E.H., J.L.S., J.J.S., and J.R.H. acknowledge support from an NSF-GOALI grant. J.R.H. acknowledges

support from the Alfred P. Sloan Foundation and from the Packard Foundation. C.P.C. and R.J.S. acknowledge support from the NSF. We would like to acknowledge Stan Williams for initially suggesting the possibility of an ionization process in the write step for large particle monolayers.

## References and Notes

- (1) Mirkin, C. A.; Letsinger, R. L.; Mucic, R. C.; Storhoff, J. J. *Nature* **1996**, *382*, 607.
- (2) Shiang, J. J.; Collier, C. P.; Heath, J. R. *J. Phys. Chem. B* **1998**, *102*, 3425.
- (3) Heath, J. R.; Knobler, C. M.; Leff, D. V. *J. Phys. Chem. B* **1997**, *101*, 189.
- (4) (a) Remacle, F. R.; Collier, C. P.; Heath, J. R.; Levine, R. D. *Chem. Phys. Lett.* **1998**, *291*, 453. (b) Remacle, F. R.; Collier, C. P.; Markovich, G.; Heath, J. R.; Banin, U.; Levine, R. D. *J. Phys. Chem. B* **1998**, *102*, 7727.
- (5) Corn, R. M.; Higgins, D. A. *Chem. Rev.* **1994**, *94*, 107.
- (6) Florsheimer, M.; Looser, H.; Kupfer, M.; Gunter, P. *Thin Solid Films* **1994**, *244*, 1001.
- (7) Shen, Y. R. *Annu. Rev. Chem.* **1989**, *40*, 327.
- (8) Vydra, J.; Eich, M. *Appl. Phys. Lett.* **1995**, *72*, 275.
- (9) Smolyaninov, I. I.; Zayats, A. V.; Davis, C. C. *Phys. Rev. B* **1997**, *56*, 9290.
- (10) Bozhevilyni, S. I.; Vohnsen, B.; Pedersen, K. *Opt. Commun.* **1998**, *150*, 49.
- (11) Gauderon, R.; Lukins, P. B.; Sheppard, C. J. R. *Opt. Lett.* **1998**, *23*, 1209.
- (12) Ohara, P.; Leff, D. V.; Heath, J. R.; Gelbart, W. M. *Phys. Rev. Lett.* **1995**, *75*, 3466.
- (13) The ionization of the particles must be a coherent process, as the electronic relaxation times associated with  $\omega_p$  are very short. See the following recent articles: (a) Feldstein, M. J., et al. *J. Am. Chem. Soc.* **1997**, *119*, 6638. (b) Smith, B. A.; Zhang, J. Z.; Giebel, U.; Schmid, G. *Chem. Phys. Lett.* **1997**, *270*, 139.
- (14) Zhao, X.; Ong, S.; Eisenthal, K. B. *Chem. Phys. Lett.* **1993**, *202*, 513.
- (15) Simon, M.; Trager, F.; Assion, A.; Lang, B.; Voll, S.; Gerber, G. *Chem. Phys. Lett.* **1998**, *296*, 579.
- (16) Rubahn, H.-G. *Appl. Surf. Sci.* **1997**, *109/110*, 575.
- (17) Bigot, J.-Y.; Merle, J.-C.; Cregut, O.; Daunois, A. *Phys. Rev. Lett.* **1995**, *75*, 4702.
- (18) Heilweil, E. J.; Hochstrasser, R. M. *J. Chem. Phys.* **1985**, *82*, 4762.
- (19) Roberti, T. W.; Smith, B. A.; Zhang, J. Z. *J. Chem. Phys.* **1995**, *102*, 3860.
- (20) Belotskii E. D.; Tomchuk, P. M. *Surf. Sci.* **1990**, *239*, 143, and references therein.
- (21) Smith, B. A.; Zhang, J. Z.; Griebel, U.; Schmid, G. *Chem. Phys. Lett.* **1997**, *270*, 139.
- (22) Feldstein, M. J.; Keating, C. D.; Liau, Y.; Natan, M. J.; Scherer, N. F. *J. Am. Chem. Soc.* **1997**, *119*, 6638.
- (23) Zhang, J. Z. *Acc. Chem. Res.* **1997**, *30*, 423, and references therein.